Charge transfer and surface scattering at Cu-C_{60} planar interfaces

A. F. Hebard,* R. R. Ruel, and C. B. Eom†
Bell Laboratories, Lucent Technologies, Murray Hill, New Jersey 07974
(Received 29 March 1996; revised manuscript received 16 July 1996)

Thin-film planar structures of Cu and C_{60} have been sequentially deposited onto sapphire substrates in high vacuum and studied using *in situ* resistivity measurements during deposition together with *ex situ* atomic force microscopy characterization of surface topography. Two different regimes of behavior are identified. In the first of these, the thin-film limit in which the Cu is thin enough to be in the coalescence regime with an islanded morphology, the presence of an adjacent C_{60} monolayer, doped by charge transfer from the metal, creates a shunting path and a corresponding pronounced *decrease* in resistance. The sheet resistance of *overlying* doped monolayers is found to be $\sim$8000 Ω, with a corresponding room-temperature resistivity that is a factor of 2 less than that of the three-dimensional alkali-metal-doped compounds A_3C_{60} (A=K, Rb). The enhanced conductivity of an *underlying* monolayer of C_{60} is sufficient to reduce the critical thickness at which an overlying Cu film becomes conducting by almost a factor of 2 even though the roughness of such films is enhanced over that of Cu films deposited directly on the substrate. In the second regime of behavior, the continuous film limit in which the Cu is thick enough to have a size-effect resistivity proportional to the reciprocal of the film thickness, the presence of an adjacent C_{60} monolayer gives rise to an *increase* in resistance. Measurements on a number of samples with different thicknesses reveal that this resistance increase is best described by diffuse surface scattering. A scattering cross section of 5 Å^2 resulting from a fit to this model represents the contact area under each C_{60} molecule. [S0163-1829(96)04643-7]

I. INTRODUCTION

Electronic transport in thin films is known to be strongly affected by interfacial phenomena. For example, the scattering of conduction electrons at grain boundaries or at planar interfaces defined by the top and bottom surfaces of the film under study can contribute significantly to the resistivity. If an isolated adsorbate is present on the surface, then translational symmetry parallel to the interface is broken and scattering of the conduction electrons occurs in processes where momentum is not conserved. Thus, an appreciable fraction of the conduction electrons can scatter diffusely and give rise to an additional resistance which correlates with roughness of surface topography, the presence of surface defects and imperfections, and/or the presence of foreign atoms either as adsorbates or as interstitial subsurface impurities. On the other hand, an interface with a smooth mirrorlike finish which is free of defects and adsorbates will, in a first approximation, simply reflect the conduction electrons (specular scattering) and have no effect on the resistivity. Even at nominally smooth interfaces, however, where diffuse scattering might be expected to be small, charge-transfer and chemical bonding effects can have an equally pronounced effect on electronic transport. This can happen if the metal is thin enough so that the amount of electronic charge transferred represents a significant reduction in the charge density of the metal. In reality, charge transfer and diffuse scattering cannot be simply separated. The charge transferred from a metal to an adsorbate implies charge separation and the simultaneous creation of a localized static impurity potential from which conduction electrons can scatter without conserving momentum. Alternatively, the presence of an adsorbate may induce a rearrangement of surface and near-surface bonds and thereby create a nonconducting dead layer and a corresponding increase of resistance.

Elucidation of many of these interface effects can be obtained by correlation of resistivity and structural measurements.[1,2] Such measurements are relatively easy to obtain, although interpretation can sometimes be problematic. Because of the sensitivity of transport to interface processes, a detailed understanding can only be gained by paying attention to careful sample preparation and thorough characterization. High-vacuum conditions, clean substrates, controlled source and substrate temperatures, and uniform deposition rates are minimal prerequisites for any meaningful investigation. There are extensive data in the literature[1,2] characterizing the thickness and temperature dependence of the resistivity for a variety of thin-film materials. Often, the absorption of gas molecules onto the surface of such films is observed to give rise to a resistance increase. A resistance increase as large as 30% has been reported for an $\sim$100 Å-thick Cu film covered with an adsorbed layer of CO gas molecules.[3] Explanations such as a transfer of charge from the metal to the adsorbent or a demetalization effect in which the adsorbent atoms form an insulating surface complex with the metal underlayer have been proposed but are not universally agreed upon.[1] Perhaps the most compelling explanation involves the above-mentioned scattering of conduction electrons at the interface; the adsorbed atoms give rise to diffuse scattering with a concomitant increase in resistivity that becomes particularly pronounced for small thicknesses. Fortunately, there are a number of theoretical treatments[4–7] that allow a quantitative comparison between resistance data and microscopic parameters such as the diffuse scattering probability, scattering cross sections, and lifetimes of adsorbate translations.

If C_{60} molecules rather than gas molecules are used as the adsorbent species, then uniquely different phenomenology

might be expected to occur. An obvious difference is that C_{60} can be reproducibly deposited as a thin film and therefore used as an underlayer, an overlayer, or both. Accordingly, there are two separate interfaces having properties that depend on the order of deposition.[8–10] More importantly, the C_{60} molecule has a high electron affinity and readily accepts electrons into its lowest unoccupied molecular orbital (LUMO). This is one of the reasons that the alkali-metal-doped compounds A_3C_{60} (A=K,Rb) become conductors with three electrons filling to 50% occupancy the LUMO-derived t_{1u} band in the face-centered-cubic solid.[11] Alkali metals not only have the requisite low ionization potentials that facilitate charge transfer but also have low cohesive energies, thus assuring that single ionized atoms will remain uniformly dispersed in the interstitial sites of the fcc lattice.

The higher cohesion energies of nonalkali metals which reside closer to the center of the Periodic Table favor the precipitation of metal clusters[8,10,12] resulting in phase-separated or agglomerated materials. These effects can be avoided by the fabrication of two-dimensional structures comprising sequentially deposited metal and C_{60} layers. Metals with high cohesive energies will remain intact when covered with C_{60} and multilayered Al/C_{60} structures have already been demonstrated.[8] On theoretical grounds the work functions of most metals are sufficiently low to allow the transfer of electrons from the metal to the fullerene across planar metal-fullerene interfaces.[13] Evidence that such charge transfer does indeed occur can be found, for example, in surface-enhanced Raman scattering (SERS) experiments in which the shift of the charge sensitive $A_g(2)$ pentagonal breathing mode of C_{60} molecules at the surface of a metal is found to scale in inverse proportion to the work functions of the three metals (Au, Ag, and Cu) studied.[14] Photoemission,[14,15] electron-energy-loss spectroscopy,[16] scanning-tunneling-microscopy,[17] luminescence,[18] and second-harmonic-generation studies[18] also confirm that charge transfer plays an important role at metal-fullerene interfaces. In combination, these studies suggest that there is a structural distortion of the C_{60} molecule associated with the charge transfer.

In this paper we expand on previously published reports of *in situ* resistivity measurements of C_{60}/metal multilayers and bilayers[8,19–21] in an attempt to determine in a quantitative manner the relative importance of charge transfer and surface scattering at C_{60}/metal (M) interfaces. We have directed our attention to M=Cu for several reasons: first, Cu is relatively easy to evaporate as a smooth and continuous thin film that does not readily oxidize at moderate vacuum pressures ($\leqslant 10^{-7}$ Torr), and second, there is ample evidence in the literature that charge is transferred from Cu to C_{60}. For example, in SERS experiments on C_{60}/Cu interfaces the downward shift in the $A_g(2)$ mode is comparable to the shift seen in K_3C_{60} and Rb_3C_{60} compounds,[14] thus implying that approximately three electrons are transferred to each C_{60}. This number may be somewhat less if effects due to covalency, metal-adsorbate interactions, or the polarizability of the C_{60} molecule also contribute to the Raman shift. Photoemission studies also tend to confirm a substantial charge transfer at the Cu-C_{60} interface.[14,15] Additional evidence for charge transfer is found in field-ion–scanning-tunneling-microscope (STM) measurements of C_{60} monolayers deposited onto Cu(111) surfaces. Here, the acquisition of clearly defined images of the monolayer film implies that the C_{60} layer is indeed metallic rather than semiconducting.[17] Thus the charges transferred from the Cu to the C_{60} are not localized on each molecule but rather are presumed to contribute to extended states which allow the monolayer to be conducting and hence easily imaged in the STM at low voltage.

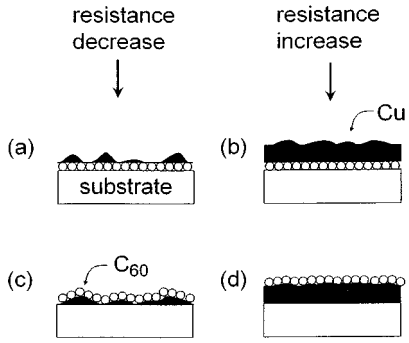

FIG. 1. Schematic summarizing the types of resistance changes observed when Cu films in different thickness regimes are in contact with C_{60} monolayers.

The central observation presented in this paper and summarized in Fig. 1 is that ultrathin Cu films exhibit a pronounced resistance *decrease* when brought into contact at either interface with a C_{60} monolayer whereas thicker Cu films show a smaller reverse effect, that is, a resistance *increase*. The crossover in behavior occurs at a Cu film thickness (~50 Å) which separates the coalescence regime, in which isolated Cu clusters begin to merge [panels (a) and (c)], from the bulk continuous regime [panels (b) and (d)], in which surface and grain-boundary scattering can have a noticeable effect on the resistivity. The resistance decrease depicted in the two left-hand panels [panels (a) and (c)] is due to charge transfer across the planar interface separating the Cu and C_{60}. The order of deposition is important. When the Cu is deposited on top of the C_{60} monolayer, which in panels (a) and (b) is depicted as ideally flat, the arriving metal atoms have an opportunity to diffuse into the C_{60} and occupy interstitial sites from which charge can be donated. If this is the case for Cu on C_{60}, as it seems to be by Raman-scattering evidence for Al on C_{60},[8] then one can expect that global conductivity can occur before the islands have coalesced [panel (a)], since the C_{60} between isolated islands is doped by interstitial Cu donor atoms. For C_{60} on top of Cu [panels (b) and (d)], the high cohesive energy of the predeposited metal prevents metal atoms from diffusing into the C_{60}, and the C_{60} is therefore doped only by the direct transfer of charge across the C_{60}-metal interface. For the ultrathin-film case depicted in panel (c), the charge is donated into extended states and the sheet resistance of the doped C_{60} monolayer is found to be on the order of 8000 Ω.

In the two right-hand panels of Fig. 1 charge transfer still occurs, but surface scattering dominates to give a resistance increase. Again, the order of deposition is important. The bilayer with Cu deposited on top of the C_{60} [panel (b)] has a rougher texture and hence a higher resistance than an equivalent Cu film deposited directly on the substrate [panel (d)]. As described in Sec. V, a quantitative estimate of the surface scattering has been obtained by studying the resistance in-

crease for C_{60}/Cu bilayers [panel (d)] with various metal thicknesses. The scattering cross section of ~ 5 Å^2 per C_{60} adsorbate molecule is consistent with the expected contact area defined by either a pentagonal or hexagonal face of the C_{60} atomic cage.

II. EXPERIMENT

All depositions and resistance measurements were performed in a stainless-steel vacuum chamber which could be pumped to a base pressure of 3×10^{-8} Torr. Temperature-controlled resistively heated boron nitride sources were configured so that each source could be independently shuttered and the evaporant fluxes separately measured with quartz-crystal microbalance monitors. A primary shutter covered the sample and was only opened after prespecified deposition rates had been established and stabilized. Thickness calibrations for each evaporant were determined in separate runs using optical profilometry. Special efforts were required to ensure a reproducible run-to-run dependence of the copper film resistivities on thickness. These efforts included the use of sapphire substrates, constant deposition rates, and the minimization, with strategically placed shielding, of thermal loading at the substrate by the evaporation sources. Unless indicated otherwise, a deposition rate of ~ 30 Å/min for Cu and ~ 10 Å/min for C_{60} was used.

The *in situ* resistivity measurements were accomplished by pre-evaporating four radially symmetric and equally spaced contacts protruding into a disk-shaped area defined by the 5-mm-diameter opening of an overlying shadow mask.[8] This mask was positioned to be in close proximity to the substrate in order to minimize regions of non-overlapping depositions from the two sources. A computer recorded the output of a four-terminal resistance bridge operating at 16 Hz and connected to the four contacts on the substrate. For resistances above 2×10^5 Ω, dc measurements were made for each current polarity with an electrometer. Four terminal van der Pauw measurements have the advantage of minimizing the effects of contact resistance in addition to providing a way to assess the spatial uniformity of the resistance.

Force microscopy on Cu/C_{60} samples was performed *ex situ* using a commercial instrument (Park Scientific Instruments SPC-400) in contact mode. The pyramidal tips had a nominal radius of 400 Å. Surface damage due to the tip was not apparent in any of the scans.

III. SINGLE-LAYER Cu AND BILAYER Cu/C_{60} FILMS

Shown in Fig. 2 is a plot of the thickness dependence of the resistivity of three Cu films deposited directly onto sapphire (solid lines) compared to four Cu films deposited directly onto an intervening underlayer of predeposited C_{60} (dashed lines). The percolation or coalescence threshold, arbitrarily defined as the thickness at which there is an onset of resistivity near 10^{-1} Ω cm is significantly less for the Cu/C_{60}/sapphire combination than it is for Cu/sapphire without the C_{60} underlayer. Similar results have been noted in earlier work on different substrates, i.e., Al/C_{60} multilayers deposited onto yttrium-stabilized zirconia (YSZ) substrates[8] and Cu/C_{60} bilayers deposited onto quartz substrates.[20]

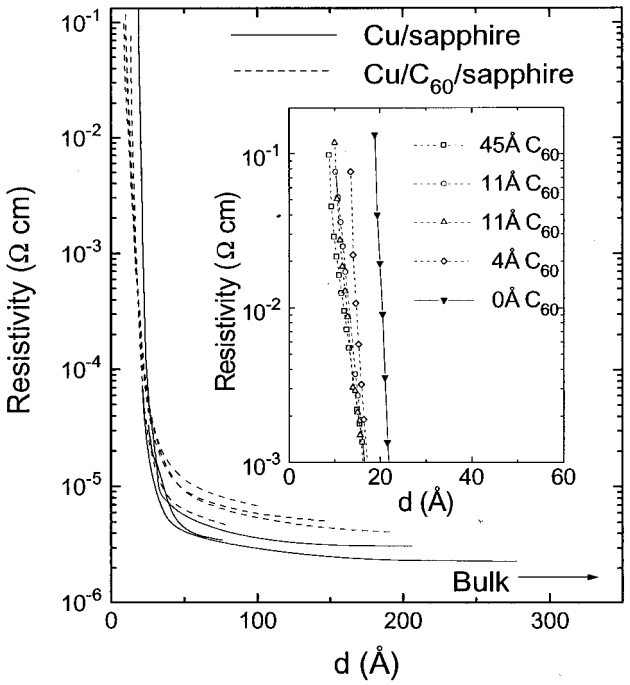

FIG. 2. Thickness dependence of the resistivity of Cu (solid lines) and Cu/C_{60} (dashed lines) deposited on sapphire. The horizontal arrow indicates the resistivity of bulk Cu. The inset shows the initial onsets in resistivity. The thickness of the underlying C_{60} layer for each of the curves is identified by the symbols in the legend.

The high-resistance region plotted in the inset of Fig. 2 shows more clearly the onsets in conductivity. The thicknesses of the C_{60} underlayer corresponding to each curve are identified in the legend. The conductivity onsets are independent of the C_{60} thickness provided this thickness is equal to or greater than a monolayer (~ 10 Å). The reduction in critical thickness defined by the 10^{-1}-Ω cm criterion, is a factor of 2, from 20 to 10 Å. The critical thickness for Cu deposited onto a partial monolayer (4 Å thickness) is seen to be at an intermediate value.

To understand this behavior, it is important to realize that film growth usually occurs in well-defined stages. Initially, metal clusters start to grow at nucleation sites and the film becomes conducting only when the clusters become sufficiently numerous and large enough to coalesce and exceed the percolation threshold for conduction. In the early stages of growth, tunneling or thermionic emission[22] can give rise to transport between isolated islands. Accordingly, the critical thickness for conduction may not be the same as the critical thickness for geometrical percolation of growing clusters. These considerations must be taken into account when trying to understand the role of the underlying C_{60} and the enhancement of the conductivity threshold. For example, the tunneling barriers between isolated Cu islands may be lower when C_{60} rather than sapphire is the substrate. Alternatively, the interface energy at the Cu/C_{60} boundary may favor the growth of smoother films which coalesce and conduct at lower coverage.[19,20] And in yet another scenario, the underlying C_{60} may become conducting, by charge donation from interstitial Cu atoms or charge donation across Cu/C_{60}

TABLE I. Summary of AFM measurements on single-layer Cu and bilayer Cu/C_{60} thin-film samples. The Cu thickness d_{Cu} is given in column one and the C_{60} layer, when present, is one monolayer thick.

d_{Cu} (Å)	C_{60} underlayer	rms roughness (Å)	peak-peak (Å)
45	No	1.60	12.7
45	Yes	4.46	38.9
60	No	1.82	13.7
60	Yes	3.06	22.7
120	No	2.12	17.4
120	Yes	4.14	30.9

interfaces, and thus create an electrical shunt in parallel with the percolating clusters.[8,19–21]

Insight into the applicability of each of these possibilities was obtained by using atomic-force microscopy (AFM) to compare the surface morphologies of Cu and Cu/C_{60} samples having the same Cu thickness. Three pairs of samples were studied with each pair having the same amount of Cu deposited onto separate substrates, one of which was covered by a predeposited C_{60} monolayer. The results, summarized in Table I, show that for the three thicknesses chosen (45, 60, and 120 Å), a film deposited onto the substrate with the predeposited C_{60} monolayer had, in all cases, a substantially rougher morphology than an equivalent film deposited directly onto the sapphire. The roughness data summarized in Table I were calculated from topographical scans such as shown in Fig. 3 for the film with Cu thickness of 60 Å. The smoother topography of the single-layer Cu film (upper panel) contrasts sharply with the rougher topography of the Cu/C_{60} bilayer (lower panel).

These AFM data thus eliminate the scenario in which interface energies between Cu and C_{60} give rise to smoother films. One can also argue, albeit with less conviction, that for the same amount of deposited Cu, the film with the rougher topography (i.e., Cu on C_{60}) should, in its initial stages of growth, comprise islands with greater near-neighbor separation and thus show lower conduction by tunneling through the substrate. The flaw in this argument is that the tunneling barrier might also be affected, i.e., the tunneling barriers between Cu and C_{60} may be reduced enough to overcome the greater island separation and thereby be responsible for the observed higher conductivity. Accordingly, the film morphology and tunneling arguments cannot be irrefutably invoked to explain the enhanced conductivity thresholds of the Cu/C_{60} bilayers. Doping of the C_{60} monolayer by charge transfer remains the most likely cause. We will return to this discussion in Secs. VI and VII.

IV. RESISTIVITIES OF CONTINUOUS THIN FILMS

The AFM scans of Fig. 3 show the surface morphologies of films that are in the continuous regime with a transport scattering length l, which exceeds the film thickness d. In this regime the film resistivity can be described by the equation

$$\rho = \rho_0 \left(1 + \frac{\alpha l_0}{d} \right), \tag{1}$$

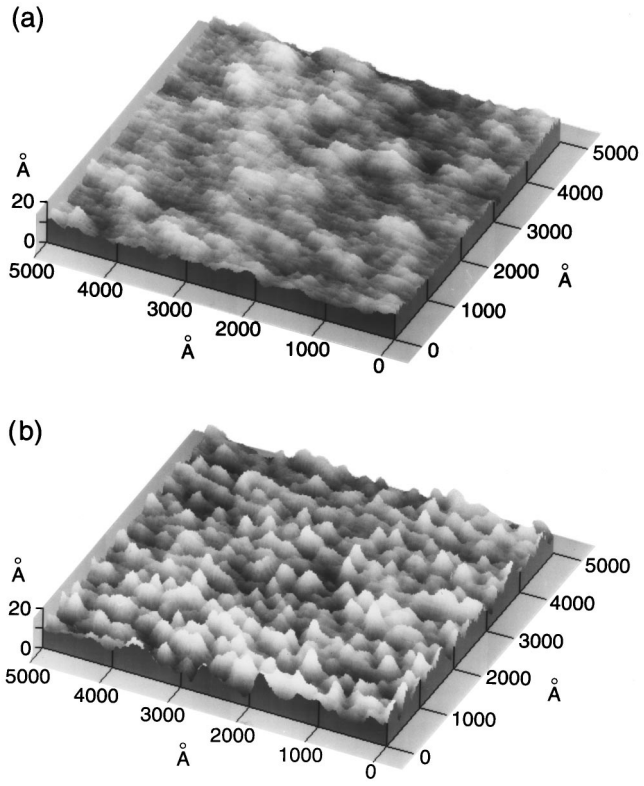

FIG. 3. AFM topographical scans of a 60-Å-thick film deposited (a) directly onto a sapphire substrate and (b) directly onto an intervening C_{60} monolayer.

where ρ_0 is the residual resistivity and α is a constant that parametrizes scattering at the grain boundaries and/or at the film surfaces. We assume that ρ_0 can be written in the Drude form, $\rho_0 = m\nu_F / ne^2 l_0$, where m is the carrier mass, n the carrier volume density, ν_F the Fermi velocity, and e the electronic charge. The d^{-1} dependence is known as the classical size effect[1] and derives from the assumption that the scattering is isotropic and can be characterized by an effective mean free path of the electrons described by the equation

$$\frac{1}{l} = \frac{1}{l_0} + \frac{\alpha}{d}. \tag{2}$$

Using this expression in the Drude equation $\rho = m\nu_F / ne^2 l$, gives Eq. (1) above.

In Fig. 4 the lower resistivity data of Fig. 1 has been replotted as a function of d^{-1}. The dashed lines are regression fits to the data in the regions where the d^{-1} dependence is apparent. For most of the films this dependence begins for thicknesses in the range of 50–70 Å. Using Eq. (1), the extracted fitting parameters provide for each film independent estimates of ρ_0 and the product $\rho_0 l_0 \alpha$. Since $\rho_0 l_0$ depends only on the carrier density, which is assumed to be the same for all films [$\rho_0 l_0 = 6.57 \times 10^{-12}\ \Omega\ \mathrm{cm}^2$ for Cu (Ref. 23)], the scattering parameter α can therefore be directly calculated. The dependence of α on ρ_0 is shown in Fig. 5.

There are a number of ways to give physical meaning to the scattering parameter α. For example, the theory of Fuchs and Sondheimer[4,5] explicitly solves the Boltzmann transport equation and in the limit $d \gg l_0$ leads to the dependence of

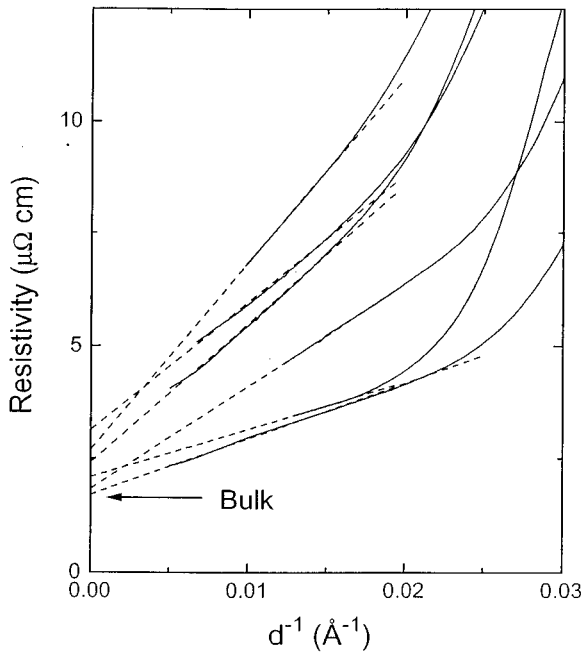

FIG. 4. Inverse thickness dependence of the resistivity of selected Cu and Cu/C_{60} samples showing for large thicknesses the linear dependence associated with the classical size effect. The dashed lines are regression fits restricted to the range of points for each curve which shows the linear dependence.

Eq. (1) with $\alpha=3(1-p)/8$. In this interpretation, p is the fraction of electrons specularly reflected at the film surfaces. In a slightly different interpretation, the theory of Mayadas and Shatzkes[6] treats scattering at the internal interfaces defined by grain boundaries of size D. In many film morphologies, $D \propto d$, and Eq. (1) therefore ensues. In a third interpretation, α can be considered as the product of an adsorbate scattering cross section σ_a and the density of adsorbate scattering centers at the surface N_a.[1] In the dilute limit, where scattering from individual adsorbates is independent, the scattering probability $1-p$ can be related to σ_a by the relation

$$1-p=N_a\sigma_a=\tfrac{8}{3}\alpha. \tag{3}$$

Thus, if monolayer coverage by a known gas gives rise to a measurable increase in α (corresponding to a decrease in the fraction of specularly reflected electrons), then the scattering cross section per adsorbed gas molecule can be readily calculated.

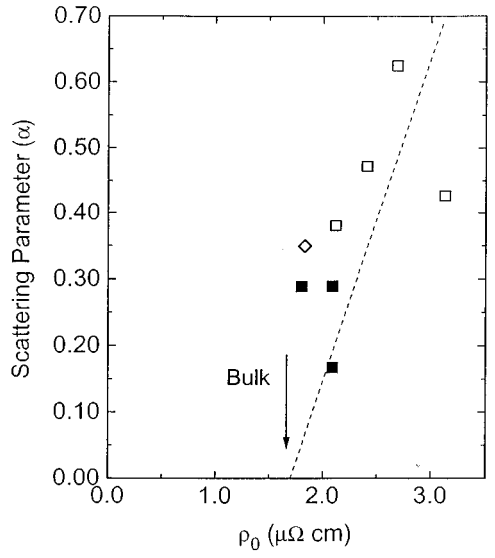

FIG. 5. Dependence of the scattering parameter α on the residual resistivity ρ_0 for eight films. The solid squares represent single-layer Cu films and the open squares represent bilayer Cu/C_{60} films having a C_{60} thickness equal to or greater than a monolayer. The open diamond refers to the bilayer sample (see Fig. 1) with submonolayer C_{60} coverage. The dashed-line fit is discussed in the text.

In Fig. 2 we note that, although the threshold for conductivity of the Cu/C_{60} bilayers occurs at a reduced thickness, there is a crossover at greater thicknesses to a region where the resistivity of the bilayers is higher than the resistivity of the single Cu layers. Similar results have been observed in previously reported measurements of Al/C_{60}/YSZ and Cu/C_{60}/quartz bilayers.[8,21] We can attribute this higher resistivity to the greater roughness observed in the AFM scans (see Fig. 4) together with additional surface scattering at the underlying Cu/C_{60} interface. This interpretation is reinforced by the data plotted in Fig. 5, which shows the dependence of α on ρ_0. The Cu/C_{60} bilayer samples (open symbols) have significantly higher scattering parameters than do the single-layer samples (solid symbols). These differences reflect a greater amount of interface scattering, both at the underlying Cu/C_{60} interface and at additional grain boundary interfaces associated with the increased film roughness. The dashed line in Fig. 5 is a regression fit to the data that is forced to include the bulk resistivity of Cu ($\alpha=0$) indicated by the vertical arrow. The off-vertical tilt of this line hints at a possible weak correlation between α and ρ_0 which is not expected on the basis of the simple transport models discussed above. This correlation is not apparent if only the rather limited data on the single layer samples (solid squares) are considered.

V. C_{60}/Cu BILAYERS: RESISTANCE INCREASE

In the previous sections, we have described the resistance changes that occur when C_{60} is present as an underlayer. When deposited as an overlayer, the interpretation of resistance changes is somewhat simplified because the strong cohesion between the predeposited metal atoms prevents diffusion of the metal atoms into the overlying C_{60} layer. Accordingly, metal atom rearrangement, if it occurs at all, is restricted to the surface layers and bulk morphology changes are negligible.

For Cu films that are thick enough to be in the classical size effect regime, the deposition of a C_{60} overlayer is observed to always give rise to a resistance increase that is usually on the order of a few percent. This phenomenology is summarized in the data of Fig. 6, which show the change in sheet resistance δR plotted as a function of C_{60} thickness. The data represent a subset of six films both with and without C_{60} underlayers. The resistance changes have been normalized to unity. In all cases the resistance changes are complete after the deposition of a monolayer (10 Å). This is true

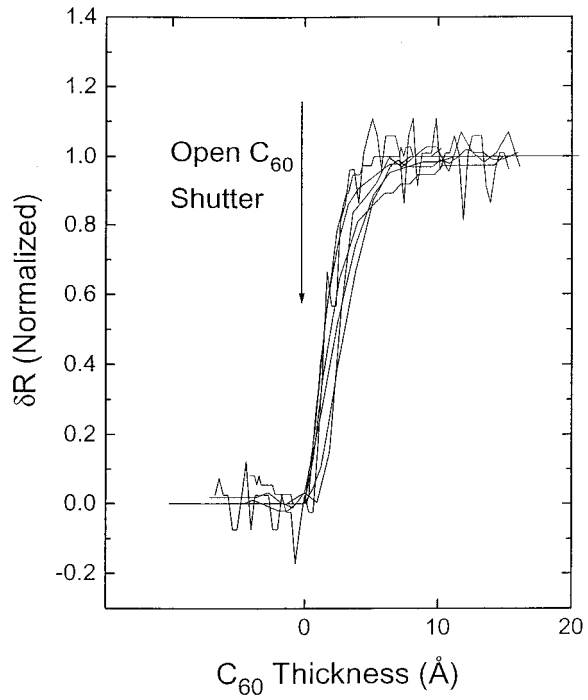

FIG. 6. Normalized change in sheet resistance plotted as a function of overlayer C_{60} thickness for seven different films. The C_{60} begins to accumulate on the substrate when the shutter is opened (vertical arrow).

for C_{60} deposition rates which vary by more than a factor of 3 in the data shown, therefore excluding the possibility that heat radiated from the deposition source is having an effect. Such a heating effect might be expected to occur upon opening the C_{60} shutter (vertical arrow). The linear onset in resistance change at the time of shutter opening precludes stress accumulation as the causative mechanism since stress effects would only be expected to occur once a significant fraction of a monolayer has formed. In like manner, the presence of a nonconducting dead layer at the surface of the metal caused by a C_{60}-induced reconstruction of surface bonds can also be excluded. At low C_{60} coverage there would only be isolated islands of nonconducting subsurface material and the effect of such islands on the conductivity would be negligeable. Finally, a possible but improbable out-diffusion of Cu atoms into the overlying monolayer and an accompanying thinning of the metal film involves too few atoms to explain the observed resistance changes. There are two remaining explanations for the resistance increase: (1) transfer of charge from the metal to the C_{60}, and (2) a change from specular to diffuse scattering at the C_{60}-metal interface. We model below each of these possibilities by using Eq. (1) to calculate the sheet resistance, $R=\rho/d$, and then finding the change in resistance δR when varying independently the charge density n and the surface scattering parameter α.

A. Charge transfer

The transfer of charge across the planar C_{60}-metal interface can, by depleting the total number of carriers in the metal, give rise to a resistance increase. When the resistivity of the Cu is near that of bulk (continuous thin-film regime),

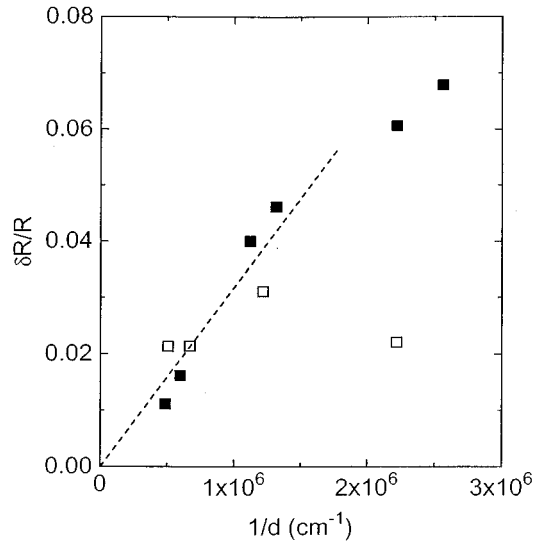

FIG. 7. Plot of $\delta R/R$ against $1/d$. The solid squares represent overcoated single-layer Cu films and the open squares represent overcoated bilayer Cu/C_{60} films. A linear dependence (dashed line) is expected from the charge-transfer model discussed in the text.

any added conductance due to the doping of the C_{60} monolayer can be ignored since the conductance of the bilayer is dominated by the Cu. This argument is validated by the results of Sec. VI below in which the doped overlying C_{60} monolayer is found to have a resistivity of $\sim 800\ \mu\Omega$ cm, a value on the order of 100 times higher than the resistivities of the bilayers considered in this section.

We begin by assuming that the sheet conductance G, of the Cu film can be written as the sum of two unperturbed contributions,

$$G=\sigma(d-\Lambda)+\sigma\Lambda, \tag{4}$$

where σ is the bulk conductivity and Λ is the thickness of the metal film adjacent to the C_{60} that is depleted of charge. Since $\sigma \propto n/\nu_F$ and $\nu_F \propto n^{1/3}$, then a change δn in n gives rise to a fractional change, $\delta\sigma/\sigma = 2\,\delta n/3n$. Only the second term of Eq. (4) is affected and we therefore can write $\delta G=\Lambda\,\delta\sigma = 2\sigma\Lambda\,\delta n/3n$, which becomes

$$\frac{\delta R}{R}=-\frac{2\,\delta N_e}{3nd} \tag{5}$$

with the substitutions $G=1/R$ and $\delta N_e=\Lambda\,\delta n$. The areal density of transferred charge, δN_e, can be easily calculated if the quantity of charge that is transferred to each C_{60} molecule is known. Thus, if the C_{60} monolayer is close packed with 10.2 Å nearest-neighbor separations, and there is one transferred electron on each molecule, then $\delta N_e = 1.11\times10^{14}$ cm^{-2}.

The applicability of the charge-transfer model as exemplified in Eq. (5) is shown in the Fig. 7 plot of $\delta R/R$ against $1/d$. The open squares represent trilayer samples, that is, C_{60}/Cu bilayers which have been deposited onto C_{60} underlayers and which therefore have a rougher morphology than the C_{60}/Cu bilayer samples (solid squares). The data are somewhat scattered and do not fit well the linear dependence described by Eq. (5). If only the four trilayer samples are

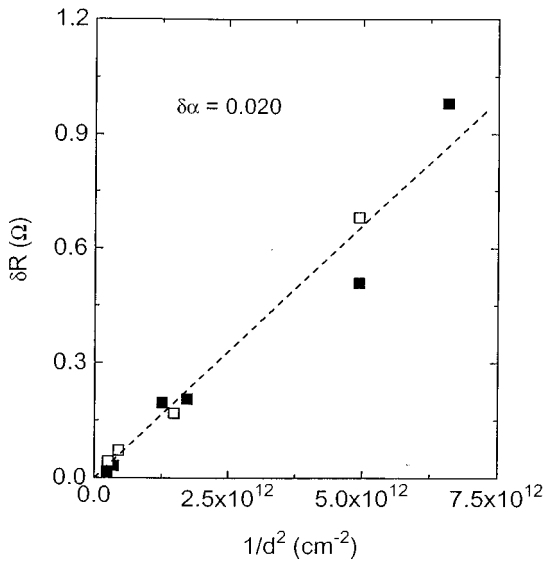

FIG. 8. Plot of δR against $1/d^2$. The solid squares represent overcoated single-layer Cu films and the open squares represent overcoated bilayer Cu/C_{60} films. A regression fit to the data yields a linear dependence (dashed line) that is consistent with the surface-scattering model discussed in the text.

considered, then $\delta R/R$ appears to be independent of d. On the other hand, if we restrict our attention to the seven samples having the largest thicknesses, then the linear regression fit (dashed line) through the origin can be interpreted with Eq. (5). Using the measured slope of 3.2×10^{-8} cm together with $n=8.5\times10^{22}$ cm^{-3} for Cu,[23] we calculate a value of δN_e that corresponds to ~35 electrons transferred to each C_{60} molecule. In previously reported work on Al-C_{60} multilayers,[8] a similar analysis implies a charge transfer of approximately six electrons to each C_{60} molecule. This is a factor of 30 larger than the 0.2 electrons per C_{60} molecule inferred from photoemission studies of Al-C_{60} interfaces.[24] Such large charge transfers, especially for C_{60} on Cu, are unphysical, and we therefore conclude that charge transfer alone is not responsible for the resistance increases that are observed.

B. Surface scattering

Changes in surface scattering associated with the presence of the overlying C_{60} molecules will become manifest in changes in the scattering parameter α. The corresponding change in R is calculated by dividing Eq. (1) by d and then taking the derivative with respect to α. The result,

$$\delta R=\frac{\rho_0 l_0}{d^2}\,\delta\alpha, \tag{6}$$

reveals a linear relation between δR and $1/d^2$ with a constant of proportionality (slope) equal to $\rho_0 l_0 \delta\alpha$. This dependence is exhibited by the data as shown in Fig. 8. We note that these are the same data that are plotted in Fig. 7 and the solid and open squares have the same meaning. In comparing the two plots we see that the data plotted with respect to the predictions of the surface scattering model display a respectable linear dependence over the whole range. This is not the case for the charge-transfer model (Fig. 7) where there is more scatter in the data, especially for the samples (open squares) in which C_{60} is deposited on Cu/C_{60} bilayers.

TABLE II. Sheet resistance R_{C60} of a monolayer of C_{60} for seven films calculated using the measured initial R_i and final R_f resistances.

R_i (Ω)	R_f (Ω)	R_{C60} (Ω)
1 200	1 013	6 500
3 319	2 572	11 430
3 345	2 332	7 700
5 574	3 437	8 964
6 458	3 270	6 624
71 830	26 740	42 600
8×10^6	8×10^6	∞

The change in scattering parameter $\delta\alpha$ can be directly calculated from the slope of the regression fit (dashed line of Fig. 8) divided by $\rho_0 l_0$ (6.57×10^{-12} Ω cm^2). The result, $\delta\alpha=0.020\pm0.004$, can be related to the scattering cross section per C_{60} adsorbate molecule, σ_a, using Eq. (3) together and the assumed areal density (1.11×10^{14} cm^{-2}) of molecules in the monolayer. We find $\sigma_a=4.8$ Å^2 or equivalently the approximate area bounded by a hexagonal or pentagonal face of the molecule. For a weak van der Waals interaction between a C_{60} molecule and a metal surface, it is not unreasonable to expect that the cross-sectional area for diffuse scattering should be approximately equal to the contact area.

VI. C_{60}/Cu BILAYERS: RESISTANCE DECREASE

In the above section we have shown that for C_{60}/Cu bilayers, surface scattering provides a better description of the resistance increase than does charge transfer. However, this does not mean that charge transfer does not occur. Specifically, it is most likely that the transfer of charge and the associated redistribution of electrons in the vicinity of each adsorbed C_{60} molecule is responsible for the observed diffuse scattering. Assuming that charge is indeed transferred from the metal to the C_{60}, it is reasonable to consider the possibility that a continuous monolayer comprising such molecules doped by transferred charge might be conducting. If this is indeed the case, then the resistance of the C_{60}/Cu bilayer will be less than that of the underlying Cu film only if the Cu film is sufficiently thin to assure that its conductance does not dominate over that of the C_{60} monolayers. Ideally, one would like to deposit a smooth Cu film with a thickness of a few atomic layers. In practice, as will be shown below, films in the coalescence regime are sufficient. In such films the resistance is dominated by interisland resistance, the scattering length is short, and the surface scattering which causes a resistance increase can be ignored.

If a thin Cu film with initial sheet resistance R_i is covered with a conducting monolayer which lowers the resistance of the bilayer to a final sheet resistance R_f, then the sheet re-

sistance of the monolayer, $R_{C_{60}}$, can be calculated from the parallel resistance formula as $R_{C_{60}}=R_iR_f/(R_i-R_f)$. The results of this procedure for seven films are shown in Table II. For films having R_i in the range 10^3–10^4 Ω, $R_{C_{60}}$ is relatively constant with a value of approximately 8000 Ω. In this region the coalescing islands are presumed to form a connected template for the overlying C_{60} which, when uniformly doped by the underlying Cu, creates a conducting shunt that reduces the resistance of the bilayer. For $R_i<10^4$ Ω, this conducting monolayer shunt has a uniform sheet resistance that is independent of the size and shape of the coalescing Cu islands. Such scale-independent behavior would be expected in a charge-transfer scenario in which only a few electrons need to be transferred to each C_{60} molecule to render the overlying monolayer conducting. The sheet resistance of this monolayer is independent of the thickness of the underlying Cu. Surprisingly, the inferred room-temperature resistivity of 800 μΩ cm for a 10-Å-thick monolayer is more than a factor of 2 smaller than that of A_3C_{60} films[25] and crystals.[26] This comparatively low resistance is somewhat unexpected for a monolayer which is disordered and not in epitaxial relationship to the underlying metal substrate.

For higher values of R_i, $R_{C_{60}}$ increases until for $R_i=8$ MΩ no decrease in resistance is observed when the C_{60} overlayer is deposited. In this region some of the Cu islands are isolated with the consequence that the overlying doped C_{60} on such islands is also isolated and thus does not make a contribution to the conductance. For thinner films with higher R_i, where coverage with a monolayer has no effect (i.e., $R_{C_{60}}\rightarrow\infty$), the film is presumably in the regime where interisland tunneling is the predominant conduction mechanism. The C_{60} between the islands is not doped because it is in direct contact with the insulating substrate and not the Cu metal. In this interpretation, the tunneling barriers between isolated islands are not lowered by the presence of C_{60}. This inference for C_{60}/Cu bilayers should also hold for the Cu/C_{60} bilayers discussed in Sec. III, i.e., the decrease in critical thickness for electrical conduction is not due to a change in tunneling barriers caused by the presence of the C_{60} but rather by charge transfer. In this case, however, in which the metal is deposited on top of the C_{60}, the charge may also be donated by interstitial metal atoms.

VII. DISCUSSION AND CONCLUSIONS

The surface scattering and charge-transfer effects described in the previous sections clearly have a marked effect on transport in multilayer metal/C_{60} structures. In accord with previous work, the general statement that can be made is that for ultrathin films the resistance of a bilayer is less than that of the metal film whereas for thicker films the opposite is true. It is important to realize that for all four C_{60}/metal combinations depicted in Fig. 1, electric charge is transferred to the C_{60}. Consequently, the doped monolayer of C_{60} is conducting and therefore always provides a shunting path which will decrease the resistance. This decrease dominates only when the Cu film is thin enough so that its conductance is low and determined by interisland connections [panels (a) and (c)]. The contribution of surface scattering and concomitant resistance increases can thus be ignored for such thin films. In the thick-film regime [panels (b) and (d)] where $R_{C60}=8000$ Ω is appreciably larger than $R=R_i$, the contribution $\delta R\propto -R^2/R_{C60}$ to the fractional change in R is negative and small. For example, the sample with the highest resistance in Fig. 8 ($R=14.4$ Ω) has an experimentally determined positive contribution, $\delta R=0.98$ Ω, due to surface scattering. The smaller negative contribution arising from the conducting C_{60} layer is calculated to be $-(14.4)^2/8000=-0.026$ Ω, a negligible correction on the order of a few tenths of a percent. Thicker films with less resistance would have an even smaller correction. Although the conductivity of the C_{60} monolayer due to charge transfer in these thicker films does not manifest itself in a measurable resistance change, it does result in charge separation at the C_{60}-metal interface which in turn makes a contribution to the scattering crossection.

In conclusion, we have shown in this work that a C_{60} monolayer in contact with a metal (Cu) surface can have a significant effect on electronic transport. The relative contributions of charge transfer and surface scattering have been quantitatively determined by varying the metal-layer thickness and the order of deposition. Interpretation of the data with respect to different theoretical models has been facilitated by AFM characterization of surface roughness and topography. Such characterization is especially important if superlattice structures[8] with smooth interfaces are to be considered. We believe that the results reported here are general and apply to other C_{60}-metal systems where similar effects have been reported in less detail.[8,19–21] Interesting questions remain. For example, recent photoemission and inverse photoemission studies of K-doped C_{60} monolayers on Ag(111) indicate a high density of states at the Fermi level.[27] Similar high densities of states could well be unique to metal-C_{60} interfaces and could thus be responsible for the high conductivity of the electron-doped monolayers reported here. It is also apparent that metals with higher (lower) work functions would be expected to contribute less (more) charge to each C_{60} molecule and thus give rise to a different conductivity of an overlying doped monolayer. An understanding of how the work function of the underlying metal correlates with the conductivity of the doped monolayer and/or the surface scattering cross section remains an open question requiring further research. Finally, it may be possible to adjust the level of doping and obtain two-dimensional superconductivity in an appropriately doped C_{60} monolayer. The transition temperature of such a two-dimensional system would be expected to be less than that of the three-dimensional A_3C_{60} compounds.

ACKNOWLEDGMENTS

The authors are indebted to W. E. Lawrence and R. G. Tobin for helpful discussions and critical insights into the physics of surface scattering. Useful comments and encouragements by R. C. Haddon and Julia M. Phillips and the technical assistance of R. H. Eick and J. H. Marshall are also appreciated.

*Present address: Department of Physics, University of Florida, 215 Williamson Hall, Gainesville, FL 32611-8440.
†Present address: Department of Mechanical Engineering and Materials Science, 221-A Hudson Hall, Durham, NC 27708-0300.
[1] P. Wissmann, in *Surface Physics*, edited by G. Höhler, Springer Tracts in Modern Physics Vol. 77 (Springer, New York, 1975).
[2] D. Schumacher, in *Surface Scattering Experiments with Conduction Electrons*, edited by G. Höhler, Springer Tracts in Modern Physics Vol. 128 (Springer, New York, 1975).
[3] R. Suhrmann, H. Ober, and G. Wedler, Z. Phys. Chem. **29**, 305 (1961).
[4] K. Fuchs, Proc. Cambridge Philos. Soc. **34**, 100 (1938).
[5] E. H. Sondheimer, Adv. Phys. **1**, 1 (1952).
[6] A. F. Mayadas and M. Shatzkes, Phys. Rev. B **1**, 1382 (1970).
[7] B. N. J. Persson, Phys. Rev. B **44**, 3277 (1991).
[8] A. F. Hebard, C. B. Eom, Y. Iwasa, K. B. Lyons, G. A. Thomas, D. H. Rapkine, R. M. Fleming, R. C. Haddon, Julia M. Phillips, J. H. Marshall, and R. H. Eick, Phys. Rev. B **30**, 17 740 (1994).
[9] T. R. Ohno, Y. Chen, S. E. Harvey, G. H. Kroll, J. H. Weaver, R. E. Haufler, and R. E. Smalley, Phys. Rev. B **44**, 13 747 (1991).
[10] T. R. Ohno, Y. Chen, S. E. Harvey, G. H. Kroll, P. J. Benning, J. H. Weaver, L. P. F. Chibante, and R. E. Smalley, Phys. Rev. B **47**, 2389 (1993).
[11] For reviews, see A. F. Hebard, Annu. Rev. Mater. Sci. **23**, 159 (1993); J. Weaver and D. M. Poirier, in *Solid State Physics*, edited by H. Ehrenreich and F. Spaepen (Academic, New York, 1994), Vol. **48**, p. 1.
[12] G. K. Wertheim and D. N. E. Buchanan, Solid State Commun. **88**, 97 (1993).
[13] E. Burstein, S. C. Erwin, M. Y. Jaing, and R. P. Messmer, Phys. Scr. T **41**, 1 (1992).
[14] S. J. Chase, W. S. Bacsa, M. G. Mitch, L. J. Pilione, and J. S. Lannin, Phys. Rev. B **46**, 7873 (1992).
[15] J. E. Rowe, P. Rudolf, L. H. Tjeng, R. A. Malic, G. Meigs, and C. T. Chen, Int. J. Mod. Phys. B **6**, 3909 (1992).
[16] S. Modesti, S. Cerasari, and P. Rudolf, Phys. Rev. Lett. **71**, 2469 (1963).
[17] T. Hashizume, K. Motai, X. D. Wang, H. Shinohara, Y. Saito, Y. Maruyama, K. Ohno, Y. Kawazoe, Y. Nishina, H. W. Pickering, Y. Kuk, and T. Sakurai, Phys. Rev. Lett. **18**, 2959 (1993).
[18] W. Zhao, L.-Q. Chen, Y.-X. Li, T.-N. Zhao, Y.-Z. Huang, Z.-X. Zhang, H.-T. Wang, P.-X. Ye, and Z.-X. Zhao, Spectrochem. Acta A **50**, 1759 (1994).
[19] X. D. Zhang, W. B. Zhao, K. Wu, Z. Y. Ye, J. L. Zhang, C. Y. Li, D. L. Yin, Z. N. Gu, X. H. Zhou, and Z. X. Jin, Chem. Phys. Lett. **228**, 100 (1994).
[20] W. B. Zhao, J. Chen, K. Wu, J. L. Zhang, C. Y. Li, D. L. Yin, Z. N. Gu, X. H. Zhou, and Z. X. Jin, J. Phys. Condens. Matter **6**, L631 (1994).
[21] A. F. Hebard, C.-B. Eom, R. C. Haddon, Julia M. Phillips, and J. H. Marshall, in *Proceedings of the Symposium on Fullerenes and Related Materials* (Materials Research Society, Pittsburgh, 1994).
[22] A. Golan, Y. Shapira, and M. Eizenberg, J. Vac. Sci. Technol. B **11**, 567 (1993).
[23] These values are calculated using free electron parameters for Cu: e.g., N. W. Ashcroft and N. D. Mermin, *Solid State Physics* (Holt, Rinehart, and Winston, New York, 1976), p. 38.
[24] D. W. Owens, C. M. Aldao, D. M. Poirier, and J. H. Weaver, Phys. Rev. B **51**, 17 068 (1995).
[25] A. F. Hebard, T. T. M. Palstra, R. C. Haddon, and R. M. Fleming, Phys. Rev. B **48**, 9945 (1993).
[26] X.-D. Xiang, J. G. Hou, G. Briceño, W. A. Vareka, R. Mostovoy, A. Zettl, V. H. Crespi, and M. L. Cohen, Science **256**, 1190 (1990).
[27] L. H. Tjeng, A. C. L. Heesels, R. Hesper, A. Heeres, H. T. Jonkman, and G. A. Sawatzky (unpublished).